Global expansion and redistribution of *Aedes*-borne virus transmission risk with climate change

Sadie J. Ryan[1,2,3*†], Colin J. Carlson[4,5*], Erin A. Mordecai[6], Leah R. Johnson[7]

Affiliations:

[1]Department of Geography, University of Florida, Gainesville, Florida, United States of America

[2] Emerging Pathogens Institute, University of Florida, Gainesville, Florida, United States of America

[3] School of Life Sciences, University of KwaZulu-Natal, Durban, South Africa

[4] Department of Biology, Georgetown University, Washington, DC 2007, U.S.A.

[5] National Socio-Environmental Synthesis Center, University of Maryland, Annapolis, Maryland 21401, U.S.A.

[6] Department of Biology, Stanford University, 371 Serra Mall, Stanford, California, United States of America

[7] Department of Statistics, Virginia Polytechnic and State University, 250 Drillfield Drive, Blacksburg, Virginia, United States of America

***These authors share lead author status.**

[†] **Corresponding author:** sjryan@ufl.edu

Abstract: Forecasting the impacts of climate change on *Aedes*-borne viruses—especially dengue, chikungunya, and Zika—is a key component of public health preparedness. We apply an empirically parameterized Bayesian transmission model of *Aedes*-borne viruses for the two vectors *Aedes aegypti* and *Ae. albopictus* as a function of temperature to predict cumulative monthly global transmission risk in current climates, and compare with projected risk in 2050 and 2080 based on general circulation models (GCMs). Our results show that if mosquito range shifts track optimal temperatures for transmission (26-29 °C), we can expect poleward shifts in *Aedes*-borne virus distributions. However, the differing thermal niches of the two vectors produce different patterns of shifts under climate change. More severe climate change scenarios produce proportionally worse population exposures from *Ae. aegypti*, but not from *Ae. albopictus* in the most extreme cases. Expanding risk of transmission from both mosquitoes will likely be a serious problem, even in the short term, for most of Europe; but significant reductions are also expected for *Aedes albopictus*, most noticeably in southeast Asia and west Africa. Within the next century, nearly a billion people are threatened with new exposure to both *Aedes* spp. in the worst-case scenario; but massive net losses in risk are noticeable for *Ae. albopictus*, especially in terms of year-round transmission, marking a global shift towards more seasonal risk across regions. Many other complicating factors (like mosquito range limits and viral evolution) exist, but overall our results indicate that while climate change will lead to both increased and new exposures to vector-borne disease, the most extreme increases in *Ae. albopictus* transmission are predicted to occur at intermediate climate change scenarios.

Author Summary: The established scientific consensus indicates that climate change will severely exacerbate the risk and burden of *Aedes*-transmitted viruses, including dengue, chikungunya, Zika, West Nile virus, and other significant threats to global health security. Here, we show that the story is more complicated, first and foremost due to differences between the more heat-tolerant *Aedes aegypti* and the more heat-limited *Ae. albopictus.* Almost a billion people could face their first exposure to viral transmission from either mosquito in the worst-case scenario, especially in Europe and high-elevation tropical and subtropical regions. On the other hand, while year-round transmission potential from *Ae. aegypti* is likely to expand (especially in south Asia and sub-Saharan Africa), *Ae. albopictus* loses significant ground in the tropics, marking a global shift towards seasonal risk as the tropics eventually become too hot for transmission by *Ae. albopictus*. Complete mitigation of climate change to a pre-industrial baseline could protect almost a billion people from arbovirus range expansions; but middle-of-the-road mitigation may actually produce the greatest expansion in the potential for viral transmission by *Ae. albopictus*. In any scenario, mitigating climate change also shifts the burden of both dengue and chikungunya (and potentially other *Aedes* transmitted viruses) from higher-income regions back onto the tropics, where transmission might otherwise start to be curbed by rising temperatures.

Introduction

Climate change will almost certainly have a profound effect on the global distribution and burden of infectious diseases [1–3]. Current knowledge suggests that the range of mosquito-borne diseases could expand dramatically in response to climate change [4,5]. However, the physiological and epidemiological relationships between mosquito vectors and the environment are complex and often non-linear, and experimental work has showed an idiosyncratic relationship between warming temperatures and disease transmission [6,7]. In addition, pathogens can be vectored by related species, which may be sympatric, or several pathogens may be transmitted by the same vector. Accurately forecasting the potential impacts of climate change on *Aedes*-borne viruses—which include widespread threats like dengue and yellow fever, as well as several emerging threats like chikungunya, Zika, West Nile, and Japanese encephalitis—thus becomes a key problem for public health preparedness [4,8,9]. In this paper, we compare the roles and impact of two vectors, *Aedes aegypti* and *Ae. albopictus*, in their contribution to potential transmission landscapes in a changing climate.

The intensification and expansion of vector-borne disease is likely to be a significant threat posed by climate change to human health [2,10]. Mosquito vectors are of special concern, due to the global morbidity and mortality from diseases like malaria and dengue fever, as well as the prominent public health crises caused by (or feared from) several recently-emergent viral diseases like West Nile, chikungunya, and Zika. The relationship between climate change and mosquito-borne disease is perhaps best studied, in both experimental and modeling work, for malaria and its associated *Anopheles* vectors. While climate change could exacerbate the burden of malaria at local scales, more recent evidence challenges the “warmer-sicker world” expectation [11,12]. The optimal temperature for malaria transmission has recently been demonstrated to be much lower than previously expected [13], likely leading to net decreases in optimal habitat at continental scales in the coming decades [12].

Relative to malaria, less is known about the net impact of climate change on *Aedes*-borne diseases. At a minimum, the distribution of *Aedes* mosquitoes is projected to shift in the face of climate change, with a mix of expansions in some regions and contractions in others, and no overwhelming net global pattern of gains or losses [3,8]. Ecophysiological differences between *Aedes* vector species are likely to drive differences in thermal niches, and therefore different distributions of transmission risk [6,14], now and in the future. The consequences of those range

shifts for disease burden are therefore likely to be important, but are challenging to summarize across landscapes and pathogens. Of all *Aedes*-borne diseases, dengue fever has been most frequently modeled in the context of climate change, and several models of the potential future of dengue have been published over the last two decades, with some limited work building consensus among them [4]. Models relating temperature to vectorial capacity (the number of new infectious mosquito bites generated from a human case), and applying general circulation models (GCMs) to predict the impacts of climate change, date back to the late 1990s [5]. A study from 2002 estimated that the population at risk (PAR) from dengue would rise from 1.5 billion in 1990, to 5-6 billion by 2085, as a result of climate change [15]. A more recent study suggested that climate change alone should increase the global dengue PAR by 0.28 billion by 2050, but accounting for projected changes in global economic development (using GDP as a predictor for dengue risk) surprisingly reduces the projected PAR by 0.12 billion over the same interval [16]. Mechanistic models have shown that increases or decreases in dengue risk can be predicted for the same region based on climate models, scenario selection, and regional variability [17].

Chikungunya and Zika viruses, which have emerged more recently as a public health crisis, are less well-studied in the context of climate change. A monthly model for chikungunya in Europe, constrained by the presence of *Ae. albopictus*, found that the A1B and B1 scenarios both correspond to substantial increases in chikungunya risk surrounding the Mediterranean [18]. A similar modeling study found that dengue is likely to expand far more significantly due to climate change than Zika [9] (though epidemiological differences among these three viruses remain unresolved [19–21]). However, the combined role of climate change and El Niño has already been suggested as a possible driver of the 2016 Zika pandemic's severity [9]. Global mechanistic forecasts accounting for climate change are all but nonexistent for both chikungunya and Zika, given how recently both emerged as public health crises, and how much critical information is still lacking in the basic biology and epidemiology of both pathogens.

In this study, we apply a new mechanistic model of the spatiotemporal distribution of *Aedes*-borne viral outbreaks to resolve the role climate change could play in the emergence of diseases like dengue, chikungunya, and Zika. Whereas other mechanistic approaches often rely on methods like dynamic energy budgets to build complex biophysical models for *Aedes* mosquitoes [22,23], and subsequently (sometimes) extrapolate potential epidemiological dynamics [5], our approach uses a single basic cutoff for the thermal interval where viral

transmission is possible. The simplicity and transparency of the method masks a sophisticated underlying model that links the basic rate of reproduction R_0 for *Aedes*-borne viruses to temperature, via experimentally-determined physiological response curves for traits like biting rate, fecundity, mosquito lifespan, extrinsic incubation rate, and transmission probability [6]. The model is easily projected into geographic space by defining model-based measures of suitability and classifying each location in space as suitable or not; we take a Bayesian approach in order to account for uncertainty in the experimental data. This threshold condition defines the temperatures at which transmission is not prevented, rather than the more familiar threshold at which disease invasion is expected ($R_0 > 1$, which cannot be predicted in the absence of assumptions about vector and human population sizes and other factors). We then classify each location by suitability in each month based on already published projections for current climates in the Americas [6].

Here, we expand the framework for both *Ae. aegypti* and *Ae. albopictus* to project cumulative months of suitability in current and future (2050 and 2080) climates, and further examine how global populations at risk might change in different climate change scenarios. We explore variation among both climate model selection (general circulation models; GCMs), and potential emissions pathways described in the IPCC AR5 (representative concentration pathways; RCPs). In doing so, we provide the first mechanistic forecast for the potential future transmission risk of chikungunya and Zika, which have been forecasted primarily via phenomenological methods (like ecological niche modeling [9]). Our study is also the first to address the seasonal aspects of population at risk for *Aedes*-borne diseases in a changing climate.

Methods

The Bayesian Model

Our study presents geographic projections of published experimentally-derived mechanistic models of viral transmission by *Ae. aegypti* and *Ae. albopictus*. The approach to fit the thermal responses in a Bayesian framework and combine them to obtain the posterior distribution of R_0 as a function of these traits is described in detail in Johnson *et al.* [7] and the particular traits and fits for *Ae. aegypti* and *Ae. albopictus* are presented in Mordecai *et al.* [24]. In the original modeling study, the underlying data was compiled on transmission of dengue virus by both mosquito species, and the models for *Ae. aegypti* were subsequently validated on data compiled

for three viruses (dengue, chikungunya, and Zika). Once we obtain our posterior samples for R_0 as a function of temperature we can evaluate the probability that $R_0 > 0$ (Prob($R_0 > 0$)) at each temperature, giving a distinct curve for each mosquito species. We then define cutoff of Prob($R_0 > 0$) = α to determine our estimates of the thermal niche; here, we use $\alpha = 0.975$. This very high probability allows us to isolate a temperature window for which transmission is almost certainly not excluded; this provides a conservative approach. For *Ae. aegypti*, these bounds are 21.3—34.0 °C, and for *Ae. albopictus*, 19.9—29.4 °C.

Current & Future Climates

Current mean monthly temperature data was derived from the WorldClim dataset (www.worldclim.org) [25]. For future climates, we selected four general circulation models (GCMs) that are most commonly used by studies forecasting species distributional shifts, at a set of four representative concentration pathways (RCPs) that account for different global responses to mitigate climate change. These are the Beijing Climate Center Climate System Model (BCC-CSM1.1); the Hadley GCM (HadGEM2-AO and HadGEM2-ES); and the National Center for Atmospheric Research's Community Climate System Model (CCSM4). Each of these can respectively be forecasted for RCP 2.6, RCP 4.5, RCP 6.0 and RCP 8.5. RCP numbers correspond to increased radiation in W/m^2 by the year 2100, therefore expressing scenarios of increasing severity. (However, even these scenarios are nonlinear over time; for example, in 2050, RCP 4.5 is a more severe change than 6.0.) Climate model output data for future scenarios were acquired from the research program on Climate Change, Agriculture, and Food Security (CCAFS) web portal (http://ccafs-climate.org/data_spatial_downscaling/), part of the Consultative Group for International Agricultural Research (CGIAR). We used the model outputs created using the delta downscaling method, from the IPCC AR5. For visualizations presented in the main paper (Figure 2), we used the HadGEM2-ES model, the most commonly used GCM. The mechanistic transmission model was projected onto the climate data using the 'raster' package in R 3.1.1 ('raster'[30]). Subsequent visualizations were generated in ArcMap.

Population at Risk

To quantify a measure of risk, comparable between current and future climate scenarios, we used population count data from the Gridded Population of the World, version 4 (GPW4) [26],

predicted for the year 2015. We selected this particular population product as it is minimally modeled *a priori*, ensuring that the distribution of population on the earth's surface has not been predicted by modeled covariates that would also influence our mechanistic vector-borne disease model predictions. These data are derived from most recent census data, globally, at the smallest administrative unit available, then extrapolated to produce continuous surface models for the globe for 5-year intervals from 2000-2020. These are then rendered as globally gridded data at 30 arc-seconds; we aggregated these in R to match the climate scenario grids at 5 minute resolution (approximately 10 km^2 at the equator). We used 2015 population count as our proxy for current, and explored future risk relative to the current population counts. This prevents arbitrary demographic model-imposed patterns emerging, possibly obscuring climate-generated change. We note that these count data reflect the disparities in urban and rural patterns appropriately for this type of analysis, highlighting population dense parts of the globe. Increasing urbanization would likely amplify the patterns we see, as populations increase overall, and the lack of appropriate population projections at this scale for 30-50 years in the future obviously limits the precision of the forecasts we provide. We thus opted for a most conservative approach. We finally subdivide global populations into geographic and socioeconomic regions as used by the Global Burden of Disease studies (**Figure S1**) [28]. We used the 'fasterize' R package [29] to convert these regions into rasters with percent (out of 100) coverage at polygon edges. To calculate population at risk on a regional basis, those partial-coverage rasters were multiplied by total population grids.

Results

The current pattern of suitability suggested by our model based on mean monthly temperatures (**Figure 1**) reproduces the known or projected distributions of *Aedes*-borne viruses like dengue [30], chikungunya [30], and Zika [9,32,33] well. For both *Ae. aegypti* and *Ae. albopictus*, most of the tropics is currently optimal for viral transmission year-round, with suitability declining along latitudinal gradients. Many temperate regions are suitable for up to 6 months of the year currently, but outside the areas mapped as "suitable" by previous disease-specific distribution models, or where *Aedes* mosquitoes are established; in some cases, limited outbreaks may only happen when cases are imported from travelers (e.g. in northern Australia, where dengue is not presently endemic but outbreaks happen in suitable regions [17]; or in mid-latitude regions of the

United States, where it has been suggested that traveler cases could result in limited autochthonous transmission [31,33]). In total, our model predicts that 6.01 billion people currently live in areas suitable for *Ae. aegypti* transmission at least part of the year (i.e., 1 month or more) and 6.33 billion in areas suitable for *Ae. albopictus* transmission.

Even by 2050, warming temperatures are expected to produce dramatic expansions of *Aedes* transmission risk (**Figure 2**). For *Ae. aegypti*, the pattern is fairly straightforward: major expansions of one- or two-month transmission risk in temperate regions are paired with expansion of year-round transmission in the tropics, even into the high-elevation regions that were previously protected. *Ae. albopictus* transmission risk similarly expands majorly into temperate regions, especially high latitude parts of Eurasia and North America. But the upper thermal limits to *Ae. albopictus* transmission are passed in many places, producing major reductions in regions of seasonal risk (like North Africa) and year-round suitability (northern Australia, the Amazon basin, central Africa and southern Asia). Whereas the conventional tropical-temperate gradient of mosquito-borne transmission is preserved for *Ae. aegypti*, warming becomes so severe in the tropics that year-round *Ae. albopictus* transmission risk starts to look more unfamiliar, especially in the more extreme climate pathways. By 2080, year-round suitability for transmission by *Ae. albopictus* is mostly confined to high elevation regions, southern Africa, and the Atlantic coast of Brazil; and even *Ae. aegypti* has begun to lose some core area of year-round suitability for transmission in the Amazon basin especially.

Globally, our models suggest a net increase in population at risk from *Aedes*-borne virus exposure, closely tracking the global rise in mean temperatures (**Figure 3**). For both mosquitoes, populations at risk of any exposure will experience a major net increase by 2050, on the order of roughly half a billion people; but even then, increases are more severe for *Ae. aegypti* than for *Ae. albopictus*. But by 2080, the differences between the mosquitoes produce a different result: while more severe warming continues to increase exposure for *Ae. aegypti*, up to nearly a billion net new exposures, the most extreme expansions for *Ae. albopictus* are in middle of the road scenarios (RCP 4.5 and 6.0). For year-round exposure, net changes tell an increasingly different story between the two mosquitoes. For *Ae. aegypti*, warming temperatures lead to a net increase of roughly 100-300 million people in areas of year-round transmission potential; in contrast, in RCP 8.5 by 2080, some parts of the tropics become so warm that even *Ae. aegypti* is no longer able to transmit. But even by 2050 in the mildest scenarios, there are drastic net losses of year-

round transmission potential for *Aedes albopictus*, and these only become more severe – approaching roughly 700 million – in the warmest timelines.

Breaking these results down by region (**Table 1 & 2**) highlights just how much regional velocity of climate change is likely to determine the future landscape of global health risks. For *Ae. aegypti*, the most notable net increases in all transmission risk are in all regions of Europe, with additional notable gains in east Asia, high-elevation parts of central America and east Africa, and the United States and Canada. But increases are expected across the board except in the Caribbean, where minor net losses are expected across scenarios and years. In contrast, for *Ae. albopictus*, more regionally-specific changes are anticipated. Major gains in Europe are again expected across the board, as well as less significant increases in central America, east Africa and east Asia, and the U.S. and Canada. But major net losses in *Ae. albopictus* transmission potential are also expected in several regions, including tropical Latin America, western Africa, south Asia and most of all southeast Asia, with a net loss of nearly 125 million people at risk by 2080 in RCP 8.5. Because the upper thermal limit for *Ae. albopictus* transmission is relatively low, for western Africa and southeast Asia, the largest declines in transmission potential are expected with the largest extent of warming, while less severe warming could produce broader increases and more moderate declines in transmission potential. The difference between RCP 6.0 and 8.5 is on the order of 50 and 100 million people respectively for the two regions, highlighting just how significant the degree of mitigation will be for regional health pathways.

For year-round transmission, the patterns are again less straightforward (**Table S1 & S2**), but overall, they highlight a global shift towards more seasonal risk for both mosquitoes, especially in the warmest scenarios. For *Ae. aegypti*, some of the largest net gains in people at risk are expected in southern Africa, with additional notable increases expected in Latin America. But even for *Ae. aegypti*, which has a very high upper thermal limit, warming temperatures exceed levels suitable for year-round transmission in some cases; for example, of all pathways, RCP 4.5 leads to the most severe increases in southern Asia. Overall, almost 600 million people currently live in areas where temperatures are expected to become suitable for transmission year-round, though the net increase in year-round transmission will be much less (**Table S3**). For *Aedes albopictus*, major net losses are expected in south and southeast Asia (totaling more than 400 million people no longer at year-round risk with the most extreme warming), and additional losses are expected in east Africa and Latin America. Only the

southern part of sub-Saharan Africa consistently experiences net gains in year-round transmission risk; but gross increases are also expected in several regions, most of all east Africa, placing roughly 250 million people into areas of year-round transmission despite nearly triple that number in net losses.

We finally consider the idea of "first exposures" separately (gross gains, not accounting for losses, of any transmission risk), which may be the most epidemiologically significant form of exposure. We rank regions by these first exposures (**Table 3**), and we find that consistently the most significant new exposures are expected in Europe and east Africa for both mosquitoes. As the 2005 epidemic of chikungunya in India and the 2015 pandemic of Zika virus in the Americas highlight, arboviral introductions into naïve populations can produce atypically severe outbreaks on the order of millions of infections. This confirms fears that both Europe and East Africa may—as a consequence of climate change—be increasingly at risk from these types of black swan event outbreaks [35,36]. The current outbreak of chikungunya virus in Kenya exemplifies this expanding risk.

Discussion

The dynamics of mosquito-borne illnesses are climate-driven, and current work suggests that climate change will create massive opportunities for the expansion and intensification of *Aedes*-borne illnesses within the next century. Especially since the emergence of Zika in the Americas, many modeling studies have anticipated climate-driven emergence of dengue and chikungunya at higher latitudes [37,38] and higher elevations [39,40]. Within this literature, there have been several global studies of potential expansion [9,17,41], as well as significant focused interest in North America and Europe (perhaps reflecting geographic biases in research priorities and research institutions) [42]. The majority of this work has suggested that climate change will probably increase the global burden of morbidity and mortality from dengue and chikungunya, and therefore, that mitigation will likely improve global health outcomes [43,44]. Perhaps most concerning are fears that *Aedes*-borne viruses will be introduced into regions that have previously been unsuitable for transmission, given the potential for explosive outbreaks (like Zika in the Americas, or chikungunya in India) when viruses are first introduced into naïve populations [45]. The emergence of a Zika pandemic in the Old World [46], the establishment of

chikungunya in Europe beyond small outbreaks [18], or introduction of dengue anywhere the virus (or any given serotype) has not recently been found, is still a critical concern.

Overall, our findings support the general view that climate change will produce major expansions of *Aedes*-borne viral transmission risk. However, we also find more nuanced patterns emerging between the two species, among different climate pathways, and across localities. The largest increases in population at risk are consistently in Europe, with additional increases in high altitude regions in the tropics (eastern Africa and the northern Andes) and in the United States and Canada. These increases are expected not only for occasional exposure, but also for longer seasons of transmission, especially for *Ae. aegypti.* But mosquitoes are adapted to their existing climatic range, and while viral transmission will surely track warming temperatures into new places over some intervals, there is no reason to think warming temperatures would produce a unilateral and indefinite increase in disease transmission. Here we show that in the tropics, for *Ae. albopictus* in particular, more extreme climate pathways produce warming temperatures that exceed the suitable range for transmission in many parts of the world; and in the long term, even though total exposure may increase from both mosquitoes in our study, we predict a global shift towards seasonal regimes of exposure from *Ae. albopictus*.

As warming temperatures may begin to exceed the upper thermal bounds of transmission, this produces an unexpected problem in terms of climate change mitigation. Total mitigation (down to pre-industrial baselines) would presumably prevent this redistribution of global risk. But partial mitigation of climate change could keep *Ae. albopictus* mosquitoes within optimal thermal ranges for more of the year, and thereby produce worse epidemiological outcomes. Given the already insufficient response to curb carbon emissions and keep temperatures below the 2 °C target [47], models such as the ones we present here are probably most useful as a means to anticipate possible futures, depending on the degree of partial mitigation achieved.

These global disease futures are inherently stochastic, and the degree to which our models correspond to reality depends not only on uncertainty about climate change, but also on uncertainty about the biotic homogenization process for disease [48]. For example, reductions in transmission may be less prevalent than we expect here, as—even accounting for the velocity of climate change—viruses will probably have sufficient time to adapt to warming temperatures (within whatever evolvability they possess). Increases in transmission risk are also complicated by many factors, such as the presence or absence of *Aedes* mosquitoes, which are also

undergoing their own semi-independent range shifts facilitated by both climate change and human movement; our model already describes areas where *Ae. albopictus* and *Ae. aegypti* are absent but could be present in the future (and even now the ranges of these mosquitoes are not static). Whether expanding transmission risk leads to future establishment and viral outbreaks depends not only on disease introduction, but also on land use patterns and urbanization at regional scales, a fact that may ultimately buffer some high-elevation regions like the Andes from increased disease risk [49,50].

In addition, the applicability of these models for different combinations of vector, virus, and region depends on the nuances of vector-virus coevolution and phylogeography. The underlying data in the models we use describe dengue transmission by the two mosquitoes and can most confidently be applied to describe dengue transmission. With *Ae. aegypti*, the most commonly implicated vector of dengue, our results suggest a strong and ongoing link between warming temperatures and increased transmission [24,30]. However, the temperature-dependent transmission models were also originally validated on two additional viruses (chikungunya and Zika) and performed well, indicating coarse-scale generality. For chikungunya, the losses of *Ae. albopictus* transmission potential in south and southeast Asia are especially interesting; in that region, *Ae. albopictus* is especially common, and it vectors the introduced Indian Ocean lineage (IOL) of chikungunya (characterized by the E1-226V mutation, which increases transmission efficiency by *Ae. albopictus* specifically [51,52]). In south and southeast Asia, these results might suggest a decreased risk of chikungunya transmission in the worst climate scenarios. Further, multiple chikungunya introductions to Europe have been vectored by *Ae. albopictus* and/or have carried the E1-226V mutation, suggesting that *Ae. albopictus* expansion in Europe might correspond to increased chikungunya risk [51,53,54]. On the other hand, *Ae. aegypti* may be more relevant as a chikungunya vector in the Americas, given historical precedent from the explosive 2015 outbreak [51]. Finally, for Zika, a recent model that further empirically refined these predictions predicts a higher thermal minimum bound than for dengue virus; this model is an obvious target for expanding this type of climate change research, given major interest in anticipating Zika re-emergence [55].

In practice, these models are a first step towards an adequate understanding of potential global health futures, and the forecast horizon of these models will ultimately be determined by a number of confounding factors [56,57]. In particular, the link from transmission risk to clinical

outcomes is confounded by other health impacts of global change, including changing precipitation patterns, socioeconomic development, changing patterns of land use and urbanization, potential vector (and virus) evolution and adaptation to warming temperatures, and changing healthcare and vector management landscapes, all of which covary strongly (potentially leading to nonlinearities). Moreover, human adaptation to climate change may have just as much of an impact as mitigation in determining how risk patterns shift; for example, increased drought stress will likely encourage water storage practices that increase proximity to *Aedes* breeding habitat [58]. Together these will determine the burden of *Aedes*-borne outbreaks, in ways that determine the eventual relevance of the forecasts we present here.

Many models exist to address this pressing topic, each with different approaches to control for data limitations, confounding processes, climate model uncertainty and disease model uncertainty, different concepts of population at risk, and different preferences towards experimental, mechanistic, or phenomenological approaches. While climate change poses perhaps the most serious growing threat to global health security, the relationship between climate change and worsening clinical outcomes for *Aedes*-borne diseases is unlikely to be straightforward, and no single model will accurately predict the complex process of a global regime shift in *Aedes*-borne viral transmission. Our models only set an outer spatiotemporal bound to where transmission is thermally plausible; climate change is likely to change the risk-burden relationship at fine scales within those zones of transmission non-linearly, such that areas with shorter seasons of transmission could still experience increased overall disease burdens, or vice versa. Combining broad spatial models with finer-scale models of attack rates or outbreak size is a critical step towards bridging scales [46,59], but more broadly, research building consensus between all available models is of paramount importance [60]. This task is not limited to research on dengue and chikungunya; with several emerging flaviviruses on the horizon [61,62], and countless other emerging arboviruses likely to test the limits of public health infrastructure in coming years [63], approaches like ours that bridge the gap between experimental biology and global forecasting can be one of the foundational methods of anticipating and preparing for the next emerging global health threat.

Acknowledgements

Van Savage, Naveed Heydari, Jason Rohr, Matthew Thomas, and Marta Shocket provided helpful discussions on modeling approaches. The funders had no role in study design, data collection and analysis, decision to publish, or preparation of the manuscript.

Author Information

Correspondence and requests for materials should be addressed to S.J.R. (sjryan@ufl.edu).

References

1. Hoberg EP, Brooks DR. Evolution in action: climate change, biodiversity dynamics and emerging infectious disease. Phil Trans R Soc B. 2015;370: 20130553.

2. Lafferty KD. The ecology of climate change and infectious diseases. Ecology. 2009;90: 888–900.

3. Escobar LE, Romero-Alvarez D, Leon R, Lepe-Lopez MA, Craft ME, Borbor-Cordova MJ, et al. Declining Prevalence of Disease Vectors Under Climate Change. Sci Rep. 2016;6.

4. Messina JP, Brady OJ, Pigott DM, Golding N, Kraemer MU, Scott TW, et al. The many projected futures of dengue. Nat Rev Microbiol. 2015;13: 230–239.

5. Patz JA, Martens W, Focks DA, Jetten TH. Dengue fever epidemic potential as projected by general circulation models of global climate change. Environ Health Perspect. 1998;106: 147.

6. Mordecai E, Cohen J, Evans MV, Gudapati P, Johnson LR, Lippi CA, et al. Detecting the impact of temperature on transmission of Zika, dengue, and chikungunya using mechanistic models. PLoS Negl Trop Dis. 2017;11: e0005568.

7. Johnson LR, Ben-Horin T, Lafferty KD, McNally A, Mordecai E, Paaijmans KP, et al. Understanding uncertainty in temperature effects on vector-borne disease: a Bayesian approach. Ecology. 2015;96: 203–213.

8. Campbell LP, Luther C, Moo-Llanes D, Ramsey JM, Danis-Lozano R, Peterson AT. Climate change influences on global distributions of dengue and chikungunya virus vectors. Phil Trans R Soc B. 2015;370: 20140135.

9. Carlson CJ, Dougherty ER, Getz W. An ecological assessment of the pandemic threat of Zika virus. PLoS Negl Trop Dis. 2016;10: e0004968.

10. Githeko AK, Lindsay SW, Confalonieri UE, Patz JA. Climate change and vector-borne diseases: a regional analysis. Bull World Health Organ. 2000;78: 1136–1147.

11. Ibelings B, Gsell A, Mooij W, Van Donk E, Van Den Wyngaert S, Domis D, et al. Chytrid infections and diatom spring blooms: paradoxical effects of climate warming on fungal epidemics in lakes. Freshw Biol. 2011;56: 754–766.

12. Ryan SJ, McNally A, Johnson LR, Mordecai EA, Ben-Horin T, Paaijmans K, et al. Mapping physiological suitability limits for malaria in Africa under climate change. Vector-Borne Zoonotic Dis. 2015;15: 718–725.

13. Mordecai EA, Paaijmans KP, Johnson LR, Balzer C, Ben-Horin T, Moore E, et al. Optimal temperature for malaria transmission is dramatically lower than previously predicted. Ecol Lett. 2013;16: 22–30.

14. Brady OJ, Golding N, Pigott DM, Kraemer MU, Messina JP, Reiner Jr RC, et al. Global temperature constraints on Aedes aegypti and Ae. albopictus persistence and competence for dengue virus transmission. Parasit Vectors. 2014;7: 338.

15. Hales S, De Wet N, Maindonald J, Woodward A. Potential effect of population and climate changes on global distribution of dengue fever: an empirical model. The Lancet. 2002;360: 830–834.

16. Åström C, Rocklöv J, Hales S, Béguin A, Louis V, Sauerborn R. Potential distribution of dengue fever under scenarios of climate change and economic development. Ecohealth. 2012;9: 448–454.

17. Williams C, Mincham G, Faddy H, Viennet E, Ritchie S, Harley D. Projections of increased and decreased dengue incidence under climate change. Epidemiol Infect. 2016; 1–10.

18. Fischer D, Thomas SM, Suk JE, Sudre B, Hess A, Tjaden NB, et al. Climate change effects on Chikungunya transmission in Europe: geospatial analysis of vector's climatic suitability and virus' temperature requirements. Int J Health Geogr. 2013;12: 51.

19. Funk S, Kucharski AJ, Camacho A, Eggo RM, Yakob L, Murray LM, et al. Comparative analysis of dengue and Zika outbreaks reveals differences by setting and virus. PLoS Negl Trop Dis. 2016;10: e0005173.

20. Bastos L, Villela DA, Carvalho LM, Cruz OG, Gomes MF, Durovni B, et al. Zika in Rio de Janeiro: assessment of basic reproductive number and its comparison with dengue. BioRxiv. 2016; 055475.

21. Riou J, Poletto C, Boëlle P-Y. A comparative analysis of Chikungunya and Zika transmission. Epidemics. 2017;

22. Kearney M, Porter WP, Williams C, Ritchie S, Hoffmann AA. Integrating biophysical models and evolutionary theory to predict climatic impacts on species' ranges: the dengue mosquito Aedes aegypti in Australia. Funct Ecol. 2009;23: 528–538.

23. Hopp MJ, Foley JA. Global-scale relationships between climate and the dengue fever vector, Aedes aegypti. Clim Change. 2001;48: 441–463.

24. Mordecai EA, Cohen JM, Evans MV, Gudapati P, Johnson LR, Lippi CA, et al. Detecting the impact of temperature on transmission of Zika, dengue, and chikungunya using mechanistic models. PLoS Negl Trop Dis. 2017;11: e0005568.

25. Hijmans RJ, Cameron SE, Parra JL, Jones PG, Jarvis A. Very high resolution interpolated climate surfaces for global land areas. Int J Climatol. 2005;25: 1965–1978.

26. Hijmans RJ, van Etten J. raster: Geographic analysis and modeling with raster data. [Internet]. 2012. Available: http://CRAN.R-project.org/package=raster

27. Center for International Earth Science Information Network (CIESIN), Columbia University. Gridded Population of the World, Version 4 (GPWv4). [Internet]. US NASA Socioeconomic Data

and Applications Center (SEDAC); 2016. Available: http://sedac.ciesin.columbia.edu/data/set/gpw-v4-population-count-adjusted-to-2015-unwpp-country-totals

28. Moran AE, Oliver JT, Mirzaie M, Forouzanfar MH, Chilov M, Anderson L, et al. Assessing the global burden of ischemic heart disease: part 1: methods for a systematic review of the global epidemiology of ischemic heart disease in 1990 and 2010. Glob Heart. 2012;7: 315–329.

29. Ross N. fasterize: High performance raster conversion for modern spatial data. [Internet]. Available: https://github.com/ecohealthalliance/fasterize

30. Bhatt S, Gething PW, Brady OJ, Messina JP, Farlow AW, Moyes CL, et al. The global distribution and burden of dengue. Nature. 2013;496: 504–507.

31. Nsoesie EO, Kraemer M, Golding N, Pigott DM, Brady OJ, Moyes CL, et al. Global distribution and environmental suitability for chikungunya virus, 1952 to 2015. Euro Surveill Bull Eur Sur Mal Transm Eur Commun Dis Bull. 2016;21.

32. Samy AM, Thomas SM, Wahed AAE, Cohoon KP, Peterson AT. Mapping the global geographic potential of Zika virus spread. Mem Inst Oswaldo Cruz. 2016;111: 559–560.

33. Messina JP, Kraemer MU, Brady OJ, Pigott DM, Shearer FM, Weiss DJ, et al. Mapping global environmental suitability for Zika virus. Elife. 2016;5: e15272.

34. Bogoch II, Brady OJ, Kraemer M, German M, Creatore MI, Kulkarni MA, et al. Anticipating the international spread of Zika virus from Brazil. Lancet Lond Engl. 2016;387: 335–336.

35. Flage R, Aven T. Emerging risk–Conceptual definition and a relation to black swan type of events. Reliab Eng Syst Saf. 2015;144: 61–67.

36. Musso D, Rodriguez-Morales AJ, Levi JE, Cao-Lormeau V-M, Gubler DJ. Unexpected outbreaks of arbovirus infections: lessons learned from the Pacific and tropical America. Lancet Infect Dis. 2018;

37. Ng V, Fazil A, Gachon P, Deuymes G, Radojević M, Mascarenhas M, et al. Assessment of the probability of autochthonous transmission of Chikungunya virus in Canada under recent and projected climate change. Environ Health Perspect. 2017;125.

38. Butterworth MK, Morin CW, Comrie AC. An analysis of the potential impact of climate change on dengue transmission in the southeastern United States. Environ Health Perspect. 2017;125: 579.

39. Acharya BK, Cao C, Xu M, Khanal L, Naeem S, Pandit S. Present and Future of Dengue Fever in Nepal: Mapping Climatic Suitability by Ecological Niche Model. Int J Environ Res Public Health. 2018;15: 187.

40. Equihua M, Ibáñez-Bernal S, Benítez G, Estrada-Contreras I, Sandoval-Ruiz CA, Mendoza-Palmero FS. Establishment of Aedes aegypti (L.) in mountainous regions in Mexico: increasing number of population at risk of mosquito-borne disease and future climate conditions. Acta Trop. 2017;166: 316–327.

41. Tjaden NB, Suk JE, Fischer D, Thomas SM, Beierkuhnlein C, Semenza JC. Modelling the effects of global climate change on Chikungunya transmission in the 21 st century. Sci Rep. 2017;7: 3813.

42. Tjaden NB, Caminade C, Beierkuhnlein C, Thomas SM. Mosquito-borne diseases: advances in modelling climate-change impacts. Trends Parasitol. 2017;

43. O'Neill BC, Done JM, Gettelman A, Lawrence P, Lehner F, Lamarque J-F, et al. The benefits of reduced anthropogenic climate change (BRACE): a synthesis. Clim Change. 2018;146: 287–301.

44. Colón-González FJ, Harris I, Osborn TJ, São Bernardo CS, Peres CA, Hunter PR, et al. Limiting global-mean temperature increase to 1.5–2° C could reduce the incidence and spatial spread of dengue fever in Latin America. Proc Natl Acad Sci. 2018;115: 6243–6248.

45. Lucey DR, Gostin LO. The emerging Zika pandemic: enhancing preparedness. Jama. 2016;315: 865–866.

46. Siraj AS, Perkins TA. Assessing the population at risk of Zika virus in Asia–is the emergency really over? BMJ Glob Health. 2017;2: e000309.

47. Hagel K, Milinski M, Marotzke J. The level of climate-change mitigation depends on how humans assess the risk arising from missing the 2 C target. Palgrave Commun. 2017;3: 17027.

48. Pongsiri MJ, Roman J, Ezenwa VO, Goldberg TL, Koren HS, Newbold SC, et al. Biodiversity loss affects global disease ecology. Bioscience. 2009;59: 945–954.

49. Grau HR, Aide TM, Zimmerman JK, Thomlinson JR, Helmer E, Zou X. The ecological consequences of socioeconomic and land-use changes in postagriculture Puerto Rico. AIBS Bull. 2003;53: 1159–1168.

50. Li Y, Kamara F, Zhou G, Puthiyakunnon S, Li C, Liu Y, et al. Urbanization increases Aedes albopictus larval habitats and accelerates mosquito development and survivorship. PLoS Negl Trop Dis. 2014;8: e3301.

51. Tsetsarkin KA, Chen R, Weaver SC. Interspecies transmission and chikungunya virus emergence. Curr Opin Virol. 2016;16: 143–150.

52. Tsetsarkin KA, Chen R, Leal G, Forrester N, Higgs S, Huang J, et al. Chikungunya virus emergence is constrained in Asia by lineage-specific adaptive landscapes. Proc Natl Acad Sci. 2011; 201018344.

53. Moro ML, Gagliotti C, Silvi G, Angelini R, Sambri V, Rezza G, et al. Chikungunya virus in North-Eastern Italy: a seroprevalence survey. Am J Trop Med Hyg. 2010;82: 508–511.

54. Sissoko D, Ezzedine K, Moendandzé A, Giry C, Renault P, Malvy D. Field evaluation of clinical features during chikungunya outbreak in Mayotte, 2005–2006. Trop Med Int Health. 2010;15: 600–607.

55. Tesla B, Demakovsky LR, Mordecai EA, Ryan SJ, Bonds MH, Ngonghala CN, et al. Temperature drives Zika virus transmission: evidence from empirical and mathematical models. Proc R Soc Lond B Biol Sci. 2018;285: 20180795.

56. Getz WM, Marshall CR, Carlson CJ, Giuggioli L, Ryan SJ, Romañach SS, et al. Making ecological models adequate. Ecol Lett. 2018;21: 153–166.

543 57. Petchey OL, Pontarp M, Massie TM, Kéfi S, Ozgul A, Weilenmann M, et al. The ecological
544 forecast horizon, and examples of its uses and determinants. Ecol Lett. 2015;18: 597–611.

545 58. Beebe NW, Cooper RD, Mottram P, Sweeney AW. Australia's dengue risk driven by human
546 adaptation to climate change. PLoS Negl Trop Dis. 2009;3: e429.

547 59. Perkins TA, Siraj AS, Ruktanonchai CW, Kraemer MU, Tatem AJ. Model-based projections of
548 Zika virus infections in childbearing women in the Americas. Nat Microbiol. 2016;1: 16126.

549 60. Carlson CJ, Dougherty E, Boots M, Getz W, Ryan S. Consensus and conflict among ecological
550 forecasts of Zika virus outbreaks in the United States. Sci Rep. 2018;8: 4921.

551 61. Evans MV, Murdock CC, Drake JM. Anticipating Emerging Mosquito-borne Flaviviruses in the
552 USA: What Comes after Zika? Trends Parasitol. 2018;

553 62. Olival K, Willoughby A. Prioritizing the "Dormant" Flaviviruses. EcoHealth. 2017;14: 1–2.

554 63. Gould EA, Higgs S. Impact of climate change and other factors on emerging arbovirus diseases.
555 Trans R Soc Trop Med Hyg. 2009;103: 109–121.

556

Figures and Tables

Figure 1 | Mapping current transmission risk. Maps of current monthly suitability based on mean temperatures for a temperature suitability threshold corresponding to the posterior probability that scaled $R_0 > 0$ is 97.5% for (a) *Aedes aegypti* and (b) *Aedes albopictus*, and (c) the number of people at risk (in billions) as a function of their months of exposure for *Aedes aegypti* and *Aedes albopictus.*

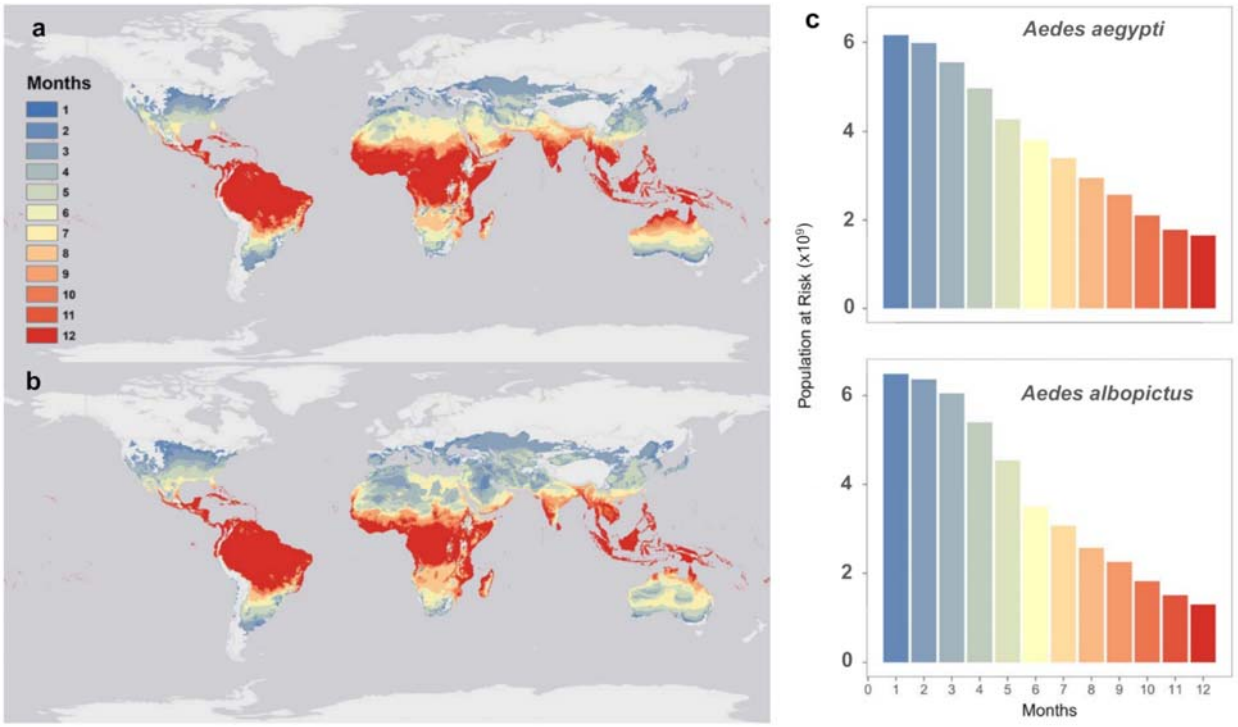

Figure 2 | Mapping future transmission risk scenarios for *Aedes aegypti and Aedes albopictus*. Maps of monthly suitability based on a temperature threshold corresponding to the posterior probability that scaled $R_0 > 0$ is greater or equal to 97.5%, for transmission by *Aedes aegypti* and *Aedes albopictus* for predicted mean monthly temperatures under current climate and future scenarios for 2050 and 2080: RCP 2.6 and RCP 8.5 in HadGEM2-ES.

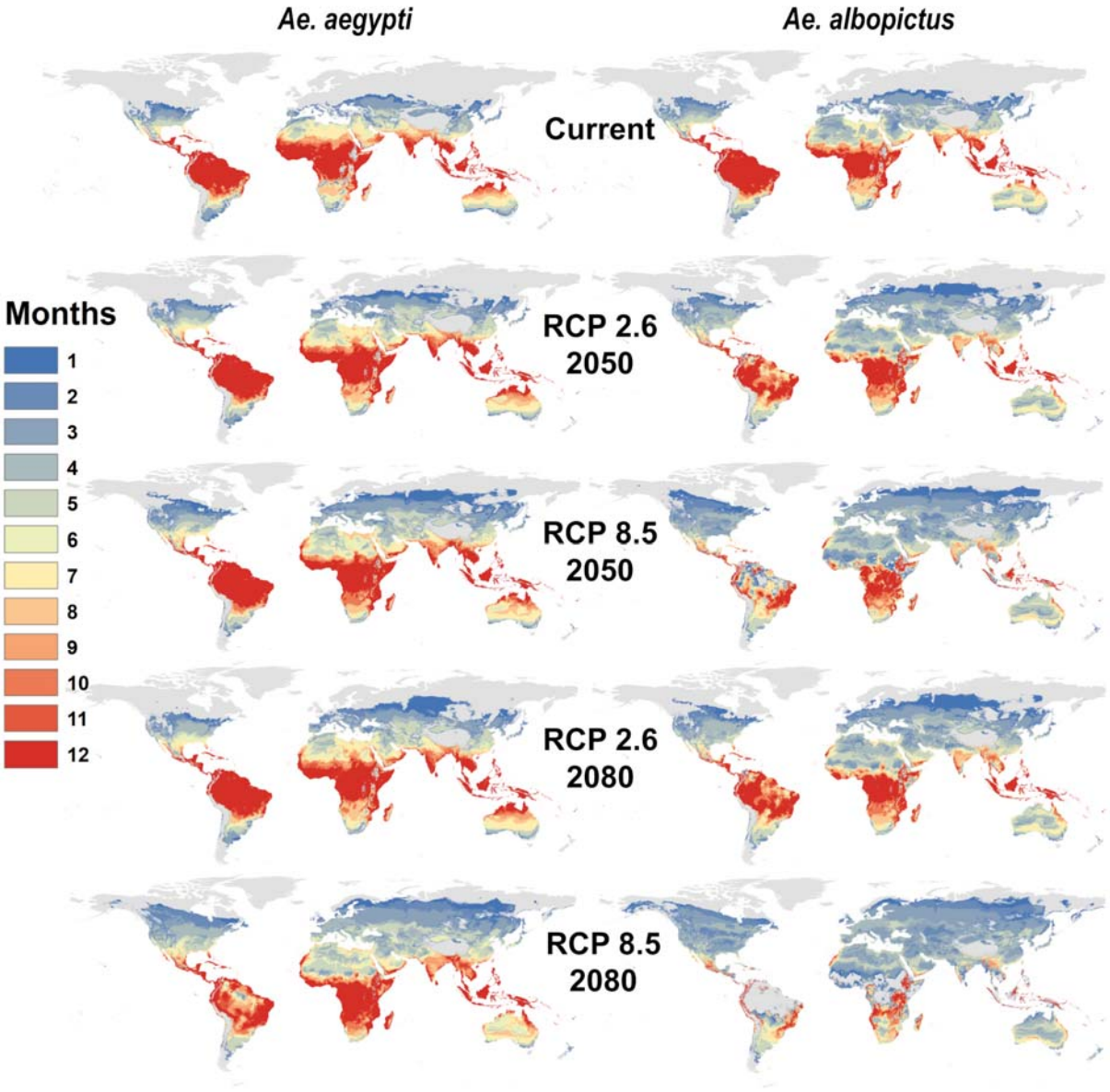

572 **Figure 3 | Projected net changes in population at risk**. Projections are given as the net
573 difference in billions at risk, for *Aedes aegypti* and *Aedes albopictus* transmission, between
574 current maps and 2050 (top row) or 2080 (bottom row). Results are further broken down by
575 representative climate pathways (RCPs), each averaged across 4 general circulation models.
576

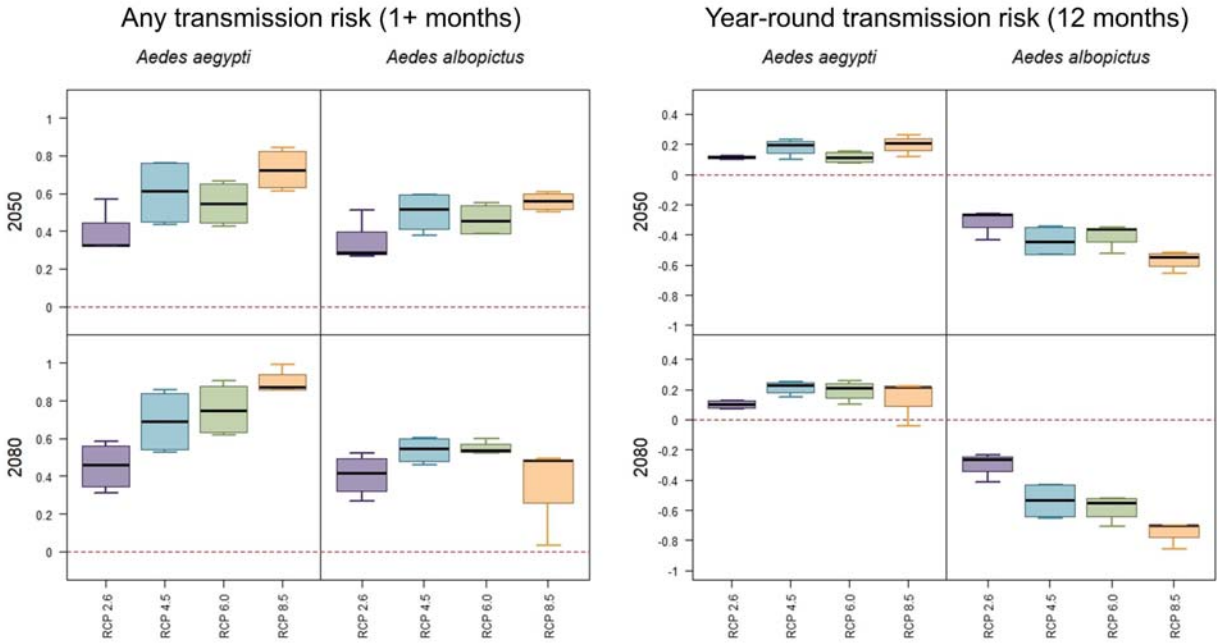

577
578
579

Table 1. Changing population at risk patterns for *Aedes aegypti.* All values are given in millions; future projections are averaged across GCMs, broken down by year (2050, 2080) and RCP (2.6, 4.5, 6.0, 8.5), and are given as net change from current population at risk. 0+/0- denote the sign of smaller non-zero values that rounded to 0.0, whereas "0" denotes true zeros.

Region	Current	2050				2080			
		2.6	4.5	6.0	8.5	2.6	4.5	6.0	8.5
Asia (Central)	69.9	8.4	10.5	9.9	12.2	8.1	11.8	12.5	15.6
Asia (East)	1,321.9	42.5	49.2	46.4	58.9	38.8	56.7	61.9	72.7
Asia (High Income Pacific)	164.0	-0.5	0+	-0.5	0.7	-0.6	0.6	1.0	1.7
Asia (South)	1,666.4	-0.1	1.6	0.7	3.7	-0.5	3.4	4.3	8.2
Asia (Southeast)	593.9	-2.1	0+	-0.6	2.3	-2.4	1.6	2.6	5.5
Australasia	12.9	3.6	5.7	5.3	6.7	4.3	6.2	6.9	8.0
Caribbean	40.4	-1.8	-1.7	-1.7	-1.6	-1.8	-1.6	-1.6	-1.5
Europe (Central)	22.7	44.2	71.8	69.0	83.3	59.0	79.3	85.5	90.6
Europe (Eastern)	41.3	57.9	110.4	93.5	133.9	80.0	124.7	130.7	156.2
Europe (Western)	114.6	47.2	132	112.0	166.8	90.3	156.4	180.8	220.9
Latin America (Andean)	31.3	2.8	3.4	3.3	4.0	2.6	3.9	4.1	5.5
Latin America (Central)	160.3	20.4	24.6	23.4	36	18.4	34.6	39.0	61.1
Latin America (Southern)	42.8	8.1	8.9	8.8	9.9	7.6	9.6	10.2	12.8
Latin America (Tropical)	181.8	19.2	19.5	19.5	19.6	18.9	19.6	19.7	19.8
North Africa & Middle East	439.5	19.7	24.1	23.8	27.2	19.3	25.9	27.3	30.3
North America (High Income)	281.9	36.2	48.3	42.6	55.0	37.8	53.6	57.1	62.8
Oceania	6.2	0.3	0.6	0.5	0.8	0.2	0.8	0.9	1.5
Sub-Saharan Africa (Central)	115.6	5.7	6.8	6.5	7.8	5.3	7.7	8.3	9.5
Sub-Saharan Africa (East)	274.8	48.8	63.7	59.1	72.2	44.7	70.8	76.6	90.9
Sub-Saharan Africa (Southern)	46.1	23.6	25.8	25.6	26.7	23.4	26.7	27.1	28.0
Sub-Saharan Africa (West)	384.0	-0.9	-0.7	-0.8	-0.7	-0.9	-0.6	-0.6	-0.4

587 **Table 2. Changing population at risk patterns for *Aedes albopictus.*** All values are given in
588 millions; future projections are averaged across GCMs, broken down by year (2050, 2080) and
589 RCP (2.6, 4.5, 6.0, 8.5), and are given as net change from current population at risk. 0+/0- denote
590 the sign of smaller non-zero values that rounded to 0.0, whereas "0" denotes true zeros.

Region	Current	2050				2080			
		2.6	4.5	6.0	8.5	2.6	4.5	6.0	8.5
Asia (Central)	75.7	5.0	6.9	6.4	8.8	4.7	8.1	9.1	11.2
Asia (East)	1,367.0	16.1	20.8	18.9	25.2	15.0	24.0	26.5	32.4
Asia (High Income Pacific)	167.7	-2.6	-2.3	-2.6	-2.0	-2.7	-2.1	-1.9	-2.8
Asia (South)	1,673.8	-3.2	-1.7	-2.3	0+	-3.5	-0.5	-0.3	-19.1
Asia (Southeast)	602.5	-5.3	-3.8	-4.0	-6.7	-5.4	-8.5	-20.1	-124.8
Australasia	16.6	3.2	3.9	3.8	4.5	3.3	4.2	4.7	5.3
Caribbean	40.8	-1.8	-1.8	-1.8	-1.8	-1.9	-1.8	-1.8	-2.3
Europe (Central)	44.8	51.3	65.0	65.1	68.3	60.6	67.8	68.9	70.7
Europe (Eastern)	70.4	84.0	116.6	104.2	123.1	101.4	122.0	123.3	129.9
Europe (Western)	135.3	98.5	179.8	161.4	208.9	149.2	199.4	215.3	243.0
Latin America (Andean)	33.9	1.6	2.2	2.0	2.6	1.6	2.6	2.7	2.5
Latin America (Central)	179.1	21.9	27.0	27.9	31.1	17.6	29.7	30.3	23.6
Latin America (Southern)	50.4	3.2	3.6	3.6	4.8	2.8	4.2	4.9	7.6
Latin America (Tropical)	203.0	-1.5	-2.0	-1.6	-6.0	-1.5	-5.6	-8.0	-26.3
North Africa & Middle East	455.0	10.6	13.0	12.9	14.2	10.4	13.5	14.1	11.8
North America (High Income)	311.6	20.6	28.4	26.0	32.1	22.6	31.6	32.3	34.7
Oceania	6.8	0.5	0.8	0.6	1.0	0.4	0.9	1.0	0.8
Sub-Saharan Africa (Central)	120.8	2.8	3.5	3.3	4.2	2.5	4.1	4.4	-3.8
Sub-Saharan Africa (East)	320.2	30.3	39.1	36.3	42.4	27.9	41.8	42.8	34.2
Sub-Saharan Africa (Southern)	70.1	3.4	3.8	3.8	3.9	3.4	4.0	4.0	4.3
Sub-Saharan Africa (West)	384.9	-1.4	-1.5	-1.5	-2.0	-1.4	-1.9	-3.5	-59.0

591

592

Table 3. Top 10 regional increases in overall transmission risk (one or more months). Regions are ranked based on millions of people exposed for the first time to any transmission risk; parentheticals give the net change (first exposures minus populations escaping transmission risk). All values are given for the worst-case scenario (RCP 8.5) in the longest term (2080).

Aedes aegypti		***Aedes albopictus***	
1. Europe (Western)	224 (220.9)	1. Europe (Western)	246.2 (243)
2. Europe (Eastern)	156.4 (156.2)	2. Europe (Eastern)	130.1 (129.9)
3. Sub-Saharan Africa (East)	92.8 (90.9)	3. Europe (Central)	71 (70.7)
4. Europe (Central)	90.9 (90.6)	4. Sub-Saharan Africa (East)	58.1 (34.2)
5. Asia (East)	81.7 (72.7)	5. Latin America (Central)	51.9 (23.6)
6. North America (High Income)	65.7 (62.8)	6. Asia (East)	41.4 (32.4)
7. Latin America (Central)	62 (61.1)	7. North America (High Income)	37.7 (34.7)
8. North Africa & Middle East	34.3 (30.3)	8. North Africa & Middle East	19.4 (11.8)
9. Sub-Saharan Africa (Southern)	28 (28)	9. Asia (South)	12.1 (-19.1)
10. Latin America (Tropical)	21.7 (19.8)	10. Asia (Central)	11.2 (11.2)
Total (across all 21 regions)	**951.3 (899.7)**	**Total** (across all 21 regions)	**721.1 (373.9)**

Supplementary Figures & Tables

Figure S1. Global health regions. We adopt the same system as the Global Burden of Disease Study in our regional breakdown.

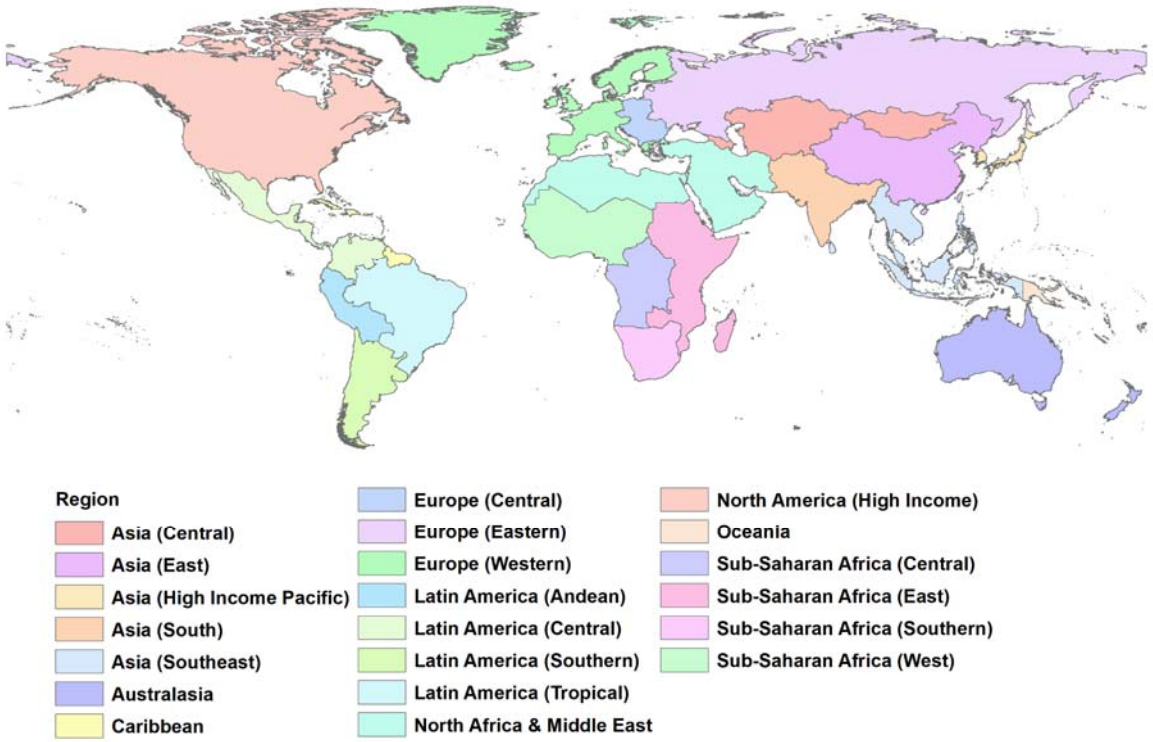

Table S1. Changing year-round (12 month) population at risk patterns for *Aedes aegypti.* All values are given in millions; future projections are averaged across GCMs, broken down by year (2050, 2080) and RCP (2.6, 4.5, 6.0, 8.5), and are given as net change from current population at risk. 0+/0- denote the sign of smaller non-zero values that rounded to 0.0, whereas "0" denotes true zeros. (Losses do not indicate loss of any transmission, only to reduction 11 or fewer months.).

Region	Current	2050				2080			
		2.6	4.5	6.0	8.5	2.6	4.5	6.0	8.5
Asia (Central)	0	0	0	0	0	0	0	0	0
Asia (East)	0+	1.4	1.8	1.1	3.7	1.6	4.5	4	8.3
Asia (High Income Pacific)	3.6	-0.2	-0.2	-0.2	-0.2	-0.2	-0.2	-0.2	-0.2
Asia (South)	286.4	21.8	71.8	13.7	73.6	12.1	89.7	72.6	29.6
Asia (Southeast)	499.4	19.2	22.4	19.9	25.1	18.9	26.3	15.4	-10.3
Australasia	0.2	0+	0+	0+	0.1	0+	0.2	0.2	0.3
Caribbean	34.8	1.8	2.2	2.1	2.8	1.7	2.6	2.9	3.3
Europe (Central)	0	0	0	0	0	0	0	0	0
Europe (Eastern)	0	0	0	0	0	0	0	0	0
Europe (Western)	0	0	0	0	0	0	0	0	0+
Latin America (Andean)	14.0	3.9	4.8	4.6	5.7	3.5	5.4	5.8	7.5
Latin America (Central)	88.1	13.0	18.8	17.0	25.8	12.0	24.4	27.4	34.1
Latin America (Southern)	0	0	0	0	0	0	0	0	0.2
Latin America (Tropical)	67.5	27.2	34.5	30.8	41.5	27.3	39	42.9	54.9
North Africa & Middle East	12.5	-5.2	-5.5	-6.0	-5.6	-4.7	-5.4	-5.4	-3.9
North America (High Income)	0.5	0.3	0.9	0.6	1.5	0.3	1.9	1.6	5.5
Oceania	0	0	0	0	0	0	0	0	0
Sub-Saharan Africa (Central)	5.3	0.3	0.6	0.4	0.9	0.3	0.7	0.9	1.7
Sub-Saharan Africa (East)	79.0	19.1	23.1	22.4	26.8	16.6	25.4	28.0	36.1
Sub-Saharan Africa (Southern)	126.9	43.8	60.7	56.7	78.3	37.9	74.3	85.5	110.3
Sub-Saharan Africa (West)	0	0+	0.1	0.1	0.3	0+	0.2	0.6	4.4

615 **Table S2. Changing year-round (12 month) population at risk patterns for *Aedes***
616 ***albopictus.*** All values are given in millions; future projections are averaged across GCMs,
617 broken down by year (2050, 2080) and RCP (2.6, 4.5, 6.0, 8.5), and are given as net change from
618 current population at risk. 0+/0- denote the sign of smaller non-zero values that rounded to 0.0,
619 whereas "0" denotes true zeros. (Losses do not indicate loss of any transmission, only to
620 reduction 11 or fewer months).

621

Region	Current	2050				2080			
		2.6	4.5	6.0	8.5	2.6	4.5	6.0	8.5
Asia (Central)	0	0	0	0	0	0	0	0	0
Asia (East)	1.3	1.4	-0.4	-0.5	-1	1	-0.9	-1	-1.2
Asia (High Income Pacific)	3.6	-0.3	-0.5	-0.4	-2.9	-0.2	-2.2	-3.1	-3.6
Asia (South)	98.3	-73	-80.3	-78.9	-87.3	-67.7	-86.1	-88.5	-92.6
Asia (Southeast)	435.3	-133.9	-213.3	-190.9	-277.4	-131.9	-254.8	-282.7	-343.6
Australasia	0.2	0+	0+	0+	0-	0+	0-	0-	0-
Caribbean	39.3	-5.9	-11.7	-9.4	-17.5	-4.5	-16.1	-18.1	-28.0
Europe (Central)	0	0	0	0	0	0	0	0	0
Europe (Eastern)	0	0	0	0	0	0	0	0	0
Europe (Western)	0	0	0	0	0+	0	0+	0+	0.1
Latin America (Andean)	17.9	2	0.1	0.5	-3	1.8	-2	-3.1	-5
Latin America (Central)	97.2	-23.2	-26.8	-25.3	-31.0	-20.8	-29.3	-31.4	-33.6
Latin America (Southern)	0	0	0	0	0+	0	0	0+	0+
Latin America (Tropical)	93.6	-0.8	-5.2	-6.1	-9.7	-2.9	-10.1	-12.9	-37.1
North Africa & Middle East	2.6	0+	0+	-0.2	-0.2	0.1	0-	-0.2	-0.1
North America (High Income)	1	2.8	1.4	1	0+	1.6	0.1	-0.2	-0.2
Oceania	0	0	0	0	0	0	0	0	0
Sub-Saharan Africa (Central)	5.9	0.4	0.4	0.5	0.1	0.4	0.1	0-	-1.4
Sub-Saharan Africa (East)	96.6	8.0	5.1	6.8	-4.5	7.5	-9.1	-9.9	-45.8
Sub-Saharan Africa (Southern)	133.5	31.9	38.8	38.8	43.4	29.7	39.5	43.9	39.2
Sub-Saharan Africa (West)	0+	0+	0.5	0.4	1.8	0+	0.9	2	6.2

622

623

Table S3. Top 10 regional increases in year-round transmission risk (12 months). Regions are ranked based on millions of people exposed for the first time to any transmission risk; parentheticals give the net change (first exposures minus populations escaping transmission risk). All values are given for the worst-case scenario (RCP 8.5) in the longest term (2080).

Aedes aegypti		***Aedes albopictus***	
1. Asia (South)	209.9 (29.6)	1. Sub-Saharan Africa (East)	114.3 (39.2)
2. Sub-Saharan Africa (East)	152.6 (110.3)	2. Latin America (Tropical)	39.7 (-37.1)
3. Latin America (Tropical)	63.2 (54.9)	3. Latin America (Central)	38.1 (-33.6)
4. Asia (Southeast)	44 (-10.3)	4. Sub-Saharan Africa (Central)	23.1 (-45.8)
5. Latin America (Central)	40.7 (34.1)	5. Asia (Southeast)	16.3 (-343.6)
6. Sub-Saharan Africa (Central)	36.6 (36.1)	6. Latin America (Andean)	8.6 (-5)
7. Sub-Saharan Africa (West)	8.7 (-130.2)	7. Sub-Saharan Africa (Southern)	6.2 (6.2)
8. Asia (East)	8.3 (8.3)	8. Sub-Saharan Africa (West)	2.5 (-194)
9. Latin America (Andean)	8 (7.5)	9. North Africa & Middle East	2.4 (-0.1)
10. North Africa & Middle East	7.4 (-3.9)	10. Oceania	2 (-1.4)
Total (across all 21 regions)	**597.2 (151.6)**	**Total** (across all 21 regions)	**256.5 (-740.8)**